

Article

Effects of Alignment of Weak Interaction Sites in Molecular Shape Recognition High-Performance Liquid Chromatography

Hiroki Noguchi ¹, Tianhang Liu ¹, Makoto Takafuji ^{1,2} and Hirotaka Ihara ^{2,3,*}

¹ Department of Applied Chemistry and Biochemistry, Kumamoto University; 2-39-1 Kurokami, Chuo-ku, Kumamoto 860-8555, Japan; 130d9219@st.kumamoto-u.ac.jp (H.N.); 168d8359@st.kumamoto-u.ac.jp (T.L.); takafuji@kumamoto-u.ac.jp (M.T.)

² Kumamoto Institute for Photo-electro Organics (PHOENICS), Kumamoto 862-0901, Japan

³ Department of New Frontier Sciences, Kumamoto University, 2-39-1 Kurokami, Chuo-ku, Kumamoto 860-8555, Japan

* Correspondence: ihara@kumamoto-u.ac.jp; Tel.: +81-96-342-3662

Academic Editor: Frank L. Dorman

Received: 18 May 2016; Accepted: 9 July 2016; Published: 24 August 2016

Abstract: This paper introduces organic phases with aligned carbonyl groups derived from L-aspartic acid, L-glutamic acid, and L- α -aminoadipic acid; their stationary phases are denoted as Sil-Asp-2C_n, Sil-Glu-2C_n, and Sil-Adi-2C_n, respectively. The stationary phases were used in high-performance liquid chromatography to investigate the alignment effect of carbonyl groups, which act as π -interaction sites, on molecular shape selectivity. The selectivities of the synthesized organic phases were evaluated using polyaromatic hydrocarbons (PAHs), including geometric isomers (e.g., *cis*- and *trans*-stilbenes). The PAH selectivities of the prepared stationary phases were higher than that of conventional octadecyl silica. Among the stationary phases prepared in this study, Sil-Glu-2C_n ($n = 18$) showed the highest selectivity toward terphenyl isomers with different twist configurations and the lowest selectivity toward planar PAHs with different aspect ratios. The results show that the molecular shape selectivity of the phases was affected by the alignment of interaction sites. As a practical application of the octadecylated amino acid derivative-bonded stationary phases, we evaluated their selectivity for tocopherol isomers and achieved good separation. Furthermore, Sil-Asp-2C_n ($n = 1$) showed hydrophilic interaction chromatography mode retention behavior for the separation of polar molecules like nucleosides.

Keywords: aspartic acid; glutamic acid; aminoadipic acid; carbonyl- π interaction; molecular shape selectivity; polyaromatic hydrocarbon; tocopherol; reversed-phase; hydrophilic interaction chromatography

1. Introduction

The development of highly selective high-performance liquid chromatography (HPLC) stationary phases is important for progress in academic and industrial fields. Surface modification of inorganic carrier materials, such as porous silica particles, with new organic phases can provide useful tools for separations. Recently, organic phases including ionic liquids [1,2], alkyl chains with embedded polar groups (EPG) [3,4], and bio-inspired phases such as organogels [5–7] and peptides [8,9] have been developed for use in HPLC. These organic phases show unique selectivities in HPLC because of their introduced specific interaction sites. Molecular ordering of the organic phase is also important for achieving a highly selective stationary phase. Although the selectivity of octadecyl silica (ODS) is mainly based on its hydrophobic distribution, dense octadecyl groups on silica increase the molecular shape selectivity of polyaromatic hydrocarbons (PAHs) and their isomers [10,11]. This selectivity

improvement is explained by highly ordered alkyl chain conformation. In addition, in the case of the polar group embedded alkyl phase, the polar group that is arranged close to the surface of silica reduces the silanol activity and improves separation of basic compound [12,13]. Furthermore, various organic phases, such as macrocyclic molecules [14,15] and helical oligoamides and -peptides [16,17], achieve specific selectivity by aligning functional groups based on their steric structure. We also found that highly ordered integration of weak interaction sites such as carbonyl groups can enhance the molecular shape selectivity of a stationary phase [18,19]. This was demonstrated by polymerization of carbonyl group-containing monomers and their crystallization on silica. The ordering of interaction sites in an organic phase with a simple chemical structure is an important approach to enhance molecular shape selectivity. In this work, we focus on the effect of the alignment of interaction sites in organic phases. We synthesize three types of carbonyl-containing molecular units derived from L-aspartic acid (Asp), L-glutamic acid (Glu), and L- α -aminoadipic acid (Adi) bonded to silica (Figure 1). The selected amino acids contain two carbonyl groups and have different numbers of methylene groups ($x = 1, 2, \text{ and } 3$) between carbonyl groups. The amino acids are hydrophobized by introduction of two octadecyl alkyl chains (C_{18}). The number of methylene groups affects the alignment of interaction sites. The purpose of this work is to investigate the effect of interaction site alignment on the molecular shape selectivity in reversed-phase HPLC. We also examine the applicability of an amino acid derivative as an organic phase in hydrophilic interaction chromatography (HILIC) by changing the length of the alkyl chains introduced on Asp.

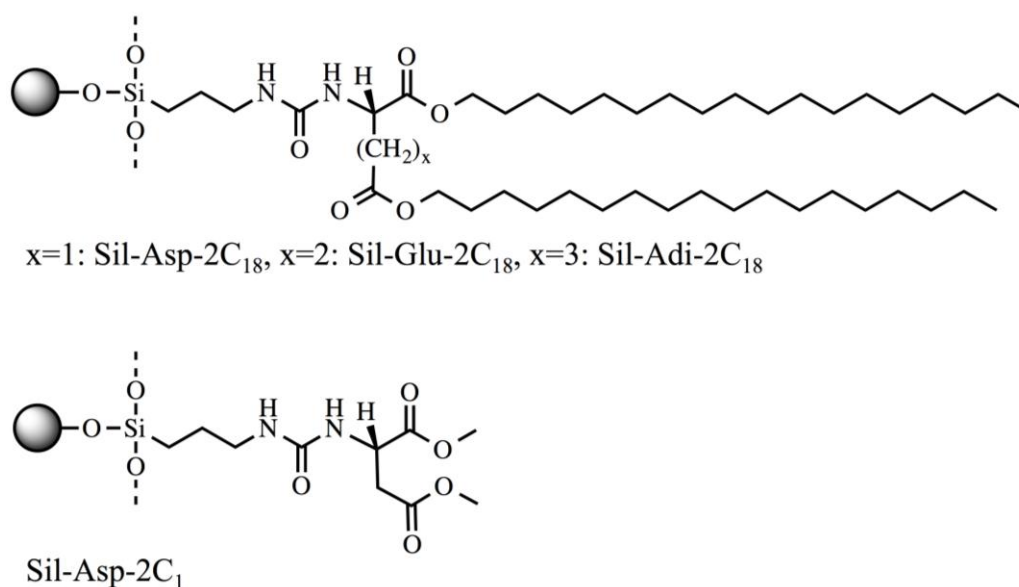


Figure 1. Chemical structures of amino acid derivative-bonded stationary phases.

2. Materials and Methods

2.1. Preparation of Amino Acid Derivatives-Bonded Stationary Phases

A typical synthetic procedure is as follows. Glu (3.00 g), stearyl alcohol (11.58 g), and *p*-toluenesulfonic acid monohydrate (12.02 g) as a catalyst were dispersed in toluene (100 mL). The mixture was stirred under reflux for 12 h in a flask with an attached Dean-Stark apparatus (FLAT Inc., Chiba, Japan). The solution was concentrated using an evaporator, and the residue was recrystallized from ethanol to give the *p*-toluenesulfonic acid salt of L-glutamic acid dioctadecylate: yield: 12.88 g (78.0%); melting point (mp): 70.6–71.4 °C. Similar procedures gave the corresponding derivatives from Asp (yield: 72.3%; mp: 88.0–90.1 °C) and Adi (yield: 75.6%; mp: 79.5–80.8 °C). Dimethyl esterification of Asp with thionyl chloride in methanol was also performed using a previously reported method [20]. The obtained diester derivatives of the amino acids were dissolved in chloroform,

neutralized with sodium hydrogen carbonate, reacted with 3-isocyanatopropyltriethoxysilane (TES) as a silane-coupling agent, and recrystallized from methanol to yield TES-Asp-2C₁₈, TES-Asp-2C₁, TES-Glu-2C₁₈, and TES-Adi-2C₁₈, where 2C₁₈ and 2C₁ correspond to dioctadecylated and dimethylated derivatives, respectively. The chemical structures of the obtained compounds were determined using ¹H nuclear magnetic resonance (NMR) and Fourier transform infrared (FT-IR) spectroscopies, and elemental analysis (EA) (See Figures S1–S11). The obtained amino acid derivatives were mixed with porous silica particles (YMC GEL SL-12S-05 silica gel, diameter 5 μm, pore size 120 Å, specific surface area 330 m²·g⁻¹) in toluene solution under reflux for 72 h to bond on the surface of the silica particles, giving Sil-Asp-2C₁₈, Sil-Asp-2C₁, Sil-Glu-2C₁₈, and Sil-Adi-2C₁₈. The amounts of amino acid derivatives that bonded to silica were determined using EA and thermogravimetric analysis (TGA).

2.2. Instrumentations

EA was performed using a Micro Corder JM10 analyzer (J-Science Lab Co., Ltd., Kyoto, Japan). FT-IR spectroscopy was performed using an FT/IR-4100 instrument (JASCO, Tokyo, Japan); a DR PRO410-M accessory (JASCO, Tokyo, Japan) was used for diffuse-reflectance infrared Fourier transform (DRIFT) spectroscopy. ¹H-NMR spectra were recorded using a Unity Inova AS400 spectrometer (Varian, Palo Alto, CA, USA) operating at 400 MHz. Chemical shifts are expressed in parts per million (ppm), and tetramethylsilane was used as an internal standard. Transmission electron microscopy (TEM) was performed using a JEM-2000× microscope (JEOL, Tokyo, Japan). TGA was performed using a SII Exstar 6000 TG/DTA 6300 thermobalance (SII, Chiba, Japan) in static air from 100 to 900 °C at a heating rate of 10 °C·min⁻¹.

2.3. Liquid Chromatography

The synthesized stationary phases were packed into stainless-steel columns that were 150 mm long with an internal diameter of 4.6 mm. A JASCO 980 pump (JASCO Corporation, Tokyo, Japan) with a Rheodyne 7725 injector (JASCO Corporation, Tokyo, Japan) (10-μL loop) and JASCO MD-2010 plus multiwavelength detector (JASCO Corporation, Tokyo, Japan) were used for liquid chromatography. The column temperature was maintained using a column jacket with a heating and cooling system. ChromNAV (version 1.14) software (JASCO Corporation, Tokyo, Japan) was used for system control and data analysis. Chromatographic-grade solvents purchased from Nacalai Tesque, Inc. (Kyoto, Japan) were used to prepare the mobile phases and samples. A commercial ODS column (GL-Science ODS-3, C: 15%, column length: 150 mm, internal diameter: 4.6 mm) (GL Science Inc., Tokyo, Japan) was used as the reference column. The retention time of methanol was used as the void volume (*t*₀) marker. The absorption of methanol was measured at 220 nm. The retention factor (*k*) was calculated from the retention time and *t*₀. The separation factor (*α*) was determined as the ratio of *k* values.

3. Results and Discussions

3.1. Evaluation of the Molecular Orientation of Organic Phases

Figure 2 shows TEM images of TES-Asp-2C₁₈, TES-Glu-2C₁₈, and TES-Adi-2C₁₈ dissolved in methanol at a concentration of 0.6 mM and then cast on a carbon-coated copper grid. The amino acid derivatives formed fibrous aggregates with diameters of around 9.5 nm in methanol. This is probably because of the biphasic structure of the 2C₁₈ derivatives based on their non-polar properties derived from the long-chain alkyl groups, and the polar urea and ester groups. It is expected that the hydrogen bonding between the carbonyl and urea groups of the amino acid derivatives support the formation of fibrous aggregates. These results suggest that the 2C₁₈ derivatives can form ordered structures on the silica particle surfaces in a HPLC mobile phase such as methanol.

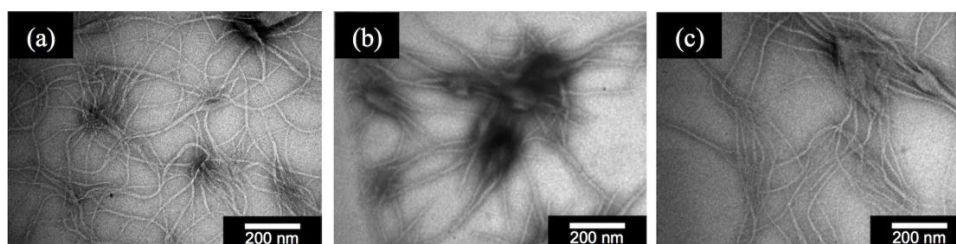


Figure 2. Transmission electron microscopy (TEM) images of nanofibrillar aggregates from (a) TES-Asp-2C₁₈: dioctadecyl ((3-(triethoxysilyl)propyl)carbamoyl)-L-aspartate; (b) TES-Glu-2C₁₈: dioctadecyl ((3-(triethoxysilyl)propyl)carbamoyl)-L-glutamate; and (c) TES-Adi-2C₁₈: dioctadecyl ((3-(triethoxysilyl)propyl)carbamoyl)-L-2-amino adipic acid in MeOH (0.6 mM). These samples were stained by 1.0 wt % uranyl acetate.

3.2. Bonding Density of Amino Acid Derivatives on Silica Surface

Bonding of the amino acid derivatives on the surface of silica was confirmed by DRIFT spectroscopy, EA and TGA. As illustrated in Figure 3, the DRIFT spectra of Sil-Asp-2C₁, Sil-Asp-2C₁₈, Sil-Glu-2C₁₈ and Sil-Adi-2C₁₈ contained peaks around 2850 and 2900 cm⁻¹, which are attributed to the C–H stretching of the long alkyl chains, and at 1650 and 1715 cm⁻¹ with a shoulder at 1745 cm⁻¹, which are characterized as C=O vibrations of urea and ester bonds, respectively. The EA results indicate that the loading amounts of carbon in the C₁₈-amino acid derivative-bonded silica samples were almost same as that of the reference ODS (C: 15%). This suggests that the density of alkyl chains on the silica surface was similar to that on the reference ODS. The C/N values of the samples were close to the theoretical values. No marked weight loss of the samples was observed after successive washing with good solvents such as chloroform. These results indicate that the amino acid derivatives were covalently bonded to the silica surface. The weight percentage (P_w) and surface coverage (N) of the bonded phases summarized in Table 1 were calculated from P_w (wt %) = $P_c M / 12 n_c$ and N ($\mu\text{mol}\cdot\text{m}^{-2}$) = $10^6 P_c / [1200 n_c - P_c M] S$, where P_c is the percentage of carbon based on the EA results, S is the specific surface area of the porous silica particles used for bonding ($330 \text{ m}^2\cdot\text{g}^{-1}$), n_c is the number of carbon atoms in a bonded molecule, and M is the molecular weight of the molecules used for bonding [21]. The thermal weight loss of the stationary phases between 100 and 900 °C (Figure S12) agrees with the EA results.

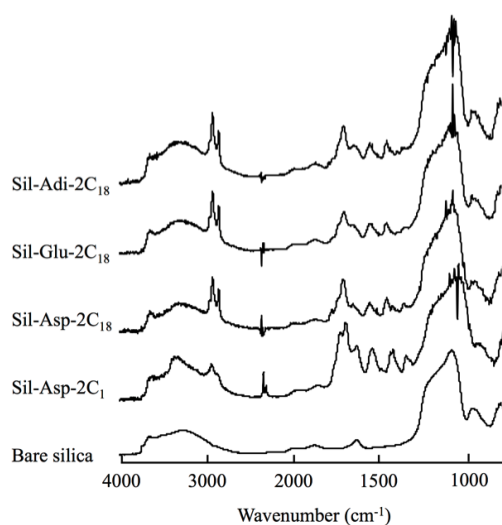


Figure 3. Comparison of diffuse-reflectance infrared Fourier transform (DRIFT) spectra of Sil-Asp-2C₁, Sil-Asp-2C₁₈, Sil-Glu-2C₁₈, Sil-Adi-2C₁₈, and bare silica.

Table 1. Bonded amount of amino acid derivatives. calcd.: Calculated value.

	%C	%N	%H	C/N		Bonded Amount		
				Found	calcd.	$\mu\text{mol}\cdot\text{m}^{-2}$	wt %	TG %
Sil-Asp-2C ₁₈	17.05	0.9	2.86	18.94	18.86	0.98	23.32	23.00
Sil-Glu-2C ₁₈	13.71	0.7	2.37	19.59	19.29	0.77	18.69	18.20
Sil-Adi-2C ₁₈	15.36	0.8	2.66	19.20	19.71	0.84	20.88	22.06
Sil-Asp-2C ₁	14.59	3.5	2.28	4.17	4.29	3.68	33.23	26.19

Theoretical C/N values and immobilized amount were calculated from C₄₄H₈₅N₂O₅ for Sil-Asp-2C₁₈, C₄₅H₈₇N₂O₅ for Sil-Glu-2C₁₈, C₄₆H₈₉N₂O₅ for Sil-Adi-2C₁₈, C₁₀H₁₇N₂O₅ for Sil-Asp-2C₁.

3.3. Reversed Phase Liquid Chromatography

Chromatographic separations were performed with the Sil-Asp-2C₁₈, Sil-Glu-2C₁₈ and Sil-Adi-2C₁₈ columns (C₁₈-amino acid derivative columns) using long-chain alkylated benzene derivatives and PAHs as solutes and methanol/water (9:1) as the mobile phase. With this sample set, the elution order of C₁₈-amino acid derivative columns followed log P values of analytes (see Figure S13). In contrast, unique separation behaviors were observed when the analytes were PAHs with characteristic structures. The molecular shape selectivity of ODS is affected by the density of alkyl chains [22]. The elution order of phenanthro[3,4-c]phenanthrene (PhPh), 1,2:3,4:5,6:7,8-tetrabenzonaphthalene (TBN), and benzo[a]pyrene (BaP) with monomeric ODS (C: 15%) is BaP ≤ PhPh < TBN, and with highly carbon loaded polymeric ODS (C: 30%) is PhPh ≤ TBN < BaP [22]. The elution orders of prepared stationary phases were different from both ODS (PhPh < BaP < TBN, see Figure 4). Because the C₁₈ amino acid derivatives were self-assemble molecules, there were possibilities that C₁₈ amino acid derivatives were bonded on the surface of silica particles locally and densely. It was supposed that the assembled structure affect for the molecular recognition. To investigate this in further detail, we clarified the molecular shape selectivities of the C₁₈-amino acid derivative columns using geometric isomers (*cis*-/*trans*-stilbenes), positional isomers with different twist angles (*o*-, *m*-, and *p*-terphenyls), and a planar compound (triphenylene), as analytes. The data in Table 2 reveal that the C₁₈-amino acid derivative columns showed higher selectivity toward planar molecules than ODS did. Sil-Glu-2C₁₈ showed the highest selectivity for *p*- and *o*-terphenyls ($\alpha = 2.46, 2.39$ and 2.03 for Sil-Glu-2C₁₈, Sil-Asp-2C₁₈ and Sil-Adi-2C₁₈, respectively), but its selectivity for triphenylene and *o*-terphenyls was lower than those of Sil-Asp-2C₁₈ and Sil-Adi-2C₁₈ ($\alpha = 2.72, 3.81$ and 2.99 for Sil-Glu-2C₁₈, Sil-Asp-2C₁₈ and Sil-Adi-2C₁₈, respectively). The length-to-breadth ratio (L/B) [23,24] is a useful indicator for evaluating molecular shape. In this work, four planar PAHs, triphenylene (L/B = 1.12), benz[a]anthracene (L/B = 1.58), chrysene (L/B = 1.72), and naphthacene (L/B = 1.89), were selected to investigate the molecular shape selectivity of the C₁₈-amino acid derivative columns. Determination of the selectivities of the columns for these molecules showed that the stationary phases with bonded C₁₈-amino acid derivatives selectively recognized molecules with higher L/B values. The naphthacene/triphenylene separation factors were the highest and lowest for Sil-Asp-2C₁₈ and Sil-Glu-2C₁₈, respectively. We also evaluated the selectivity of Sil-Asp-2C₁ using PAHs, as summarized in Table 2.

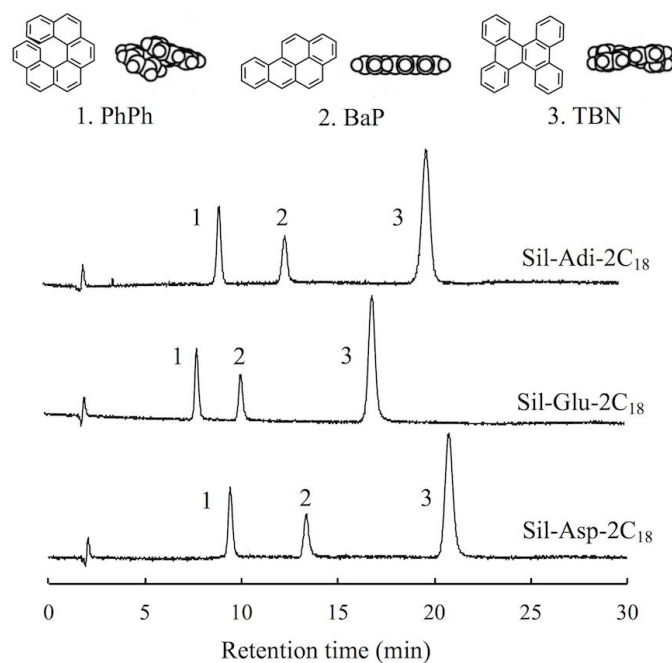


Figure 4. Chromatograms of phenanthro[3,4-c]phenanthrene (PhPh), benzo[a]pyrene (BaP) and 1,2:3,4:5,6:7,8-tetrabenzonaphthalene (TBN). Mobile phase: methanol-water (9:1), flow rate: 1.0 mL·min⁻¹, column temperature: 20 °C.

Table 2. Retention and separation factors (*k* and α) with C₁₈-amino acid derivative columns.

Analyte	Sil-Asp-2C ₁₈		Sil-Glu-2C ₁₈		Sil-Adi-2C ₁₈		ODS	
	<i>k</i>	α	<i>k</i>	α	<i>k</i>	α	<i>k</i>	α
<i>cis</i> -Stilbene	1.01	-	0.99	-	1.03	-	1.74	-
<i>trans</i> -Stilbene	1.50	1.48	1.39	1.40	1.43	1.38	1.84	1.06
<i>o</i> -Terphenyl	1.32	-	0.88	-	1.23	-	2.27	-
<i>m</i> -Terphenyl	2.45	1.86	1.88	2.14	2.12	1.72	3.22	1.42
<i>p</i> -Terphenyl	3.14	2.39	2.16	2.46	2.50	2.03	3.26	1.43
Triphenylene	5.02	3.81	2.38	2.72	3.67	2.99	3.51	1.54
Triphenylene	5.02	-	2.38	-	3.67	-	3.51	-
Benz[a]anthracene	5.66	1.13	2.56	1.07	4.05	1.10	3.73	1.06
Chrysene	5.84	1.16	2.58	1.08	4.11	1.12	3.69	1.05
Naphthacene	7.90	1.57	3.11	1.31	5.08	1.38	4.26	1.21

Mobile phase: methanol-water (9:1), flow rate: 1.0 mL·min⁻¹, column temperature: 20 °C. The α values were calculated using the *k* of the first analyte and others respectively, in each group.

To further investigate the C₁₈-amino acid derivative columns, temperature dependencies of the selectivities for triphenylene/*o*-terphenyl ($\alpha_{\text{triph}/o\text{-terp}}$) and naphthacene/triphenylene ($\alpha_{\text{naph}/\text{triph}}$) were evaluated. Figure 5 reveals that a linear plot was observed for ODS. In contrast, bending points were observed in the plots of C₁₈-amino acid derivative columns. This suggests that a steric structure change related to the molecular interaction occurred on the stationary phase. Moreover, the higher selectivities of the C₁₈-amino acid derivative columns at temperatures below 25 °C are related to temperature-dependent molecular ordering. The ordering of the molecules on the surface of the stationary phase indicates that the organic phases are locally densely bonded. This is one of the reasons for the unique selectivity of the C₁₈-amino acid derivative columns. The aligned carbonyl groups may also contribute to the molecular shape selectivity of the C₁₈-amino acid derivative columns. The number of methylene groups between the carbonyl groups of the C₁₈-amino acid derivatives is odd except for in the Glu derivative. Because of this, it is presumed that the configuration of carbonyl groups in the Glu derivative is obviously different from that of the other amino acid derivatives. The alignment of the interaction sites on Sil-Glu-2C₁₈ therefore must differ from those of the other amino acid derivatives, when it orientates on the surface of silica, and promotes recognition of the twisted structures of terphenyl isomers. For the same reason, the alignments of the interaction sites in Sil-Asp-2C₁₈ and Sil-Adi-2C₁₈ are better for recognition of planar and linear molecules than that in Sil-Glu-2C₁₈.

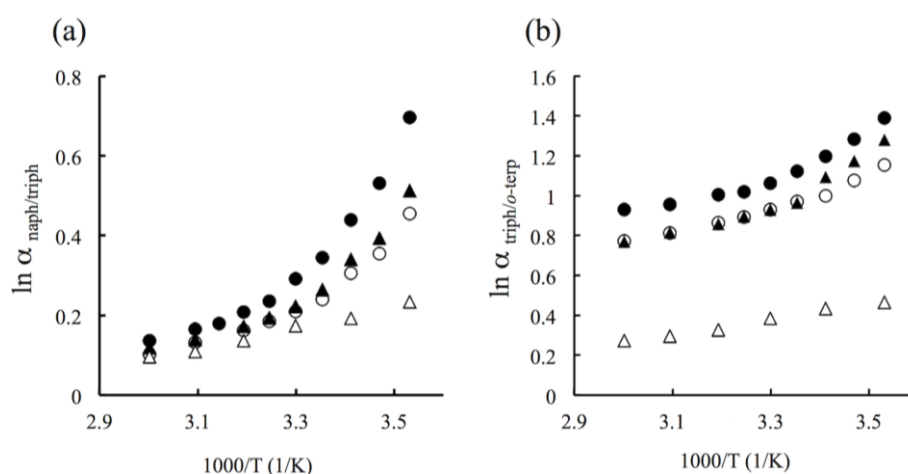


Figure 5. Van't Hoff plots for separation factor of (a) $\alpha_{\text{naph}/\text{triph}}$ and (b) $\alpha_{\text{triph}/o\text{-terp}}$ with amino acid derivatives bonded silica. Mobile phase: methanol-water (9:1), flow rate: 1.0 mL·min⁻¹. Black circle: Sil-Asp-2C₁₈, hollow circle: Sil-Glu-2C₁₈, black triangle: Sil-Adi-2C₁₈, and hollow triangle: octadecyl silica (ODS).

3.4. Hydrophilic Interaction Chromatography

The applicability of an amino acid derivative-bonded stationary phase to HILIC mode was evaluated using Sil-Asp-2C₁. The typical HILIC mode retention order was observed for phenol, resorcinol, and phloroglucinol with Sil-Asp-2C₁: higher *k* value was achieved by increasing the number of hydroxyl groups of the analyte (Table S1) [25]. Usually, a mixture of water and a polar organic solvent such as acetonitrile is used for the mobile phase in HILIC. The retention mechanism of HILIC involves liquid-liquid partitioning between the mobile phase and absorbed water on the surface of the stationary phase [26]. Thus, by increasing the content of water in the mobile phase, the retention in HILIC will decrease. Figure 6 shows the relationship between *k* and the proportion of acetonitrile in the mobile phase. Decreasing the content of acetonitrile in the mobile phase decreased the *k* values of all selected polar molecules, which is consistent with the usual retention behavior in HILIC. This is the typical HILIC mode retention behavior [25,27]. In addition, larger *k* values were obtained by molecules that show lower pK_a values (e.g., pK_a = 4.2 and 4.2 for adenine and cytosine [28]) among a sample set

(e.g., pKa = 10.5 for thymine [28]). In the HILIC, in addition to the partitioning, ion exchange between positively charged molecules and negative charged silanol also affected the retentivity. This effect may be revealed in this study.

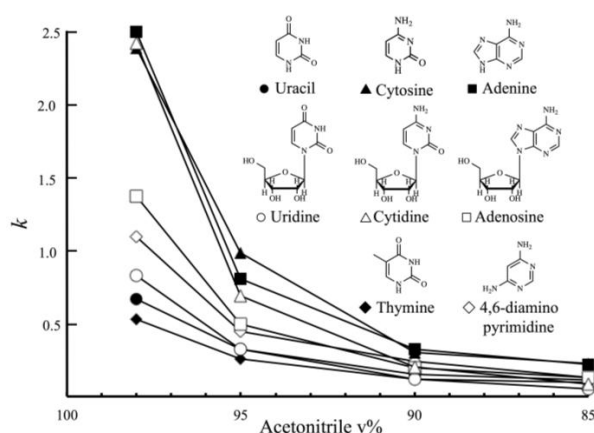


Figure 6. Effect of acetonitrile content ratio on the retention factors of polar molecules with Sil-Asp-2C₁. Mobile phase: acetonitrile and 10 mM ammonium acetate mixture, flow rate: 1.0 mL·min⁻¹, column temperature: 10 °C.

These results suggest that weak interaction site accumulation based on amino acids has the potential for application in molecular design for HILIC.

3.5. Separation of Tocopherol Isomers

Practical applications of the C₁₈-amino acid derivative columns were evaluated using the tocopherol isomers (α , β , γ , and δ isomers). Tocopherols are hydrophobic vitamins that have many beneficial bioeffects such as antioxidant and anti-inflammatory properties. For example, the importance of the role of tocopherols in retinal precursor cell differentiation is being increasingly studied [29]. Figure 7 depicts chromatograms of tocopherols obtained using the C₁₈-amino acid derivative columns and ODS. Separation of the β and γ isomers was not achieved using ODS, but was realized using the stationary phases with bonded octadecylated amino acid derivatives. In particular, Sil-Asp-2C₁₈ successfully separated all the isomers in the reversed-phase mode.

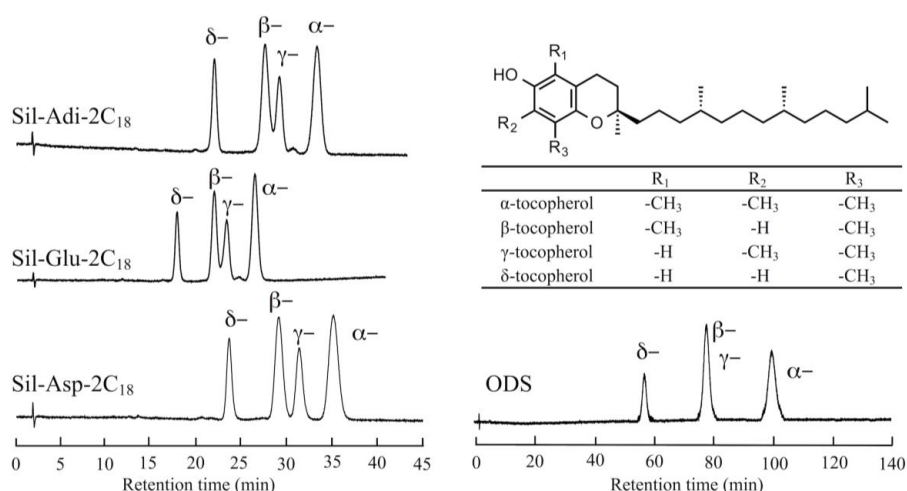


Figure 7. Chromatograms for tocopherol isomers with Sil-Asp-2C₁₈, Sil-Glu-2C₁₈, Sil-Adi-2C₁₈ and ODS. Mobile phase: methanol-water (9:1), flow rate: 1.0 mL·min⁻¹, column temperature: 10 °C.

4. Conclusions

Organic stationary phases based on Asp, Glu, and Adi with aligned carbonyl groups were synthesized and bonded on silica particles. These stationary phases showed higher molecular shape selectivities for PAHs than ODS. The highest selectivity for *p*-/*o*-terphenyl and naphthacene/*o*-terphenyl were obtained by Sil-Glu-2C₁₈ and Sil-Asp-2C₁₈, respectively. Sil-Asp-2C₁₈, Sil-Glu-2C₁₈, and Sil-Adi-2C₁₈ differ in the number of methylene groups between carbonyl groups in the original amino acids; therefore, these results indicate that the alignment of the carbonyl groups as interaction sites affects the molecular shape selectivity of these organic phases. We also evaluated the use of Sil-Asp-2C₁ as a HILIC-mode stationary phase. Like common HILIC stationary phases, Sil-Asp-2C₁ achieved higher *k* values with increasing polarity. Effective separation of tocopherol isomers was realized with the C₁₈-amino acid derivative columns in reversed-phase mode, including the separation of β and γ isomers, which could not be obtained by ODS.

Supplementary Materials: The following are available online at <http://www.mdpi.com/2297-8739/3/3/25/s1>.

Acknowledgments: This work was partially supported by Grant-in-Aid for Scientific Research and the Sasakawa Scientific Research Grant.

Author Contributions: H.I. and M.T. conceived and designed the experiments; H.N. and T.L. performed the experiments, and analyzed the data. H.N. wrote the paper and H.I. and M.T. contributed to preparation and revisions of the paper.

Conflicts of Interest: The authors declare no conflict of interest.

References

1. Sun, M.; Feng, J.; Chen, W.; Li, L.; Duan, H.; Luo, C. Improvement of the chromatographic separation performance of an imidazolium ionic liquid functionalized silica column by in situ anion-exchange with dodecyl sulfonate and dodecylbenzene sulfonate anions. *J. Sep. Sci.* **2014**, *37*, 1283–1288. [[CrossRef](#)] [[PubMed](#)]
2. Qiu, H.; Mallik, A.K.; Sawada, T.; Takafuji, M.; Ihara, H. New surface-confined ionic liquid stationary phases with enhanced chromatographic selectivity and stability by co-immobilization of polymerizable anion and cation pairs. *Chem. Commun.* **2012**, *48*, 1299–1301. [[CrossRef](#)] [[PubMed](#)]
3. Zhang, M.; Mai, W.; Zhao, L.; Guo, Y.; Qiu, H. A polar-embedded C30 stationary phase: Preparation and evaluation. *J. Chromatogr. A* **2015**, *1388*, 133–140. [[CrossRef](#)]
4. O'Sullivan, G.; Scully, N.M.; Glennon, J.D. Polar-Embedded and Polar-Endcapped Stationary Phases for LC. *Anal. Lett.* **2010**, *43*, 1609–1629. [[CrossRef](#)]
5. Noguchi, H.; Charoenraks, T.; Takafuji, M.; Ihara, H. Effects of substitution groups of glutamide-derived molecular gels on molecular shape recognition. *J. Chromatogr. A* **2015**, *1392*, 56–62. [[CrossRef](#)] [[PubMed](#)]
6. Mallik, A.K.; Qiu, H.; Takafuji, M.; Ihara, H. High molecular-shape selectivity by molecular gel-forming compounds: Bioactive and shape-constrained isomers through the integration and orientation of weak interaction sites. *Chem. Commun.* **2011**, *47*, 10341–10343. [[CrossRef](#)] [[PubMed](#)]
7. Rahman, M.M.; Takafuji, M.; Ansarian, H.R.; Ihara, H. Molecular Shape Selectivity through Multiple Carbonyl- π Interactions with Noncrystalline Solid Phase for RP-HPLC. *Anal. Chem.* **2005**, *77*, 6671–6681. [[CrossRef](#)] [[PubMed](#)]
8. Ray, S.; Takafuji, M.; Ihara, H. Chromatographic evaluation of a newly designed peptide-silica stationary phase in reverse phase liquid chromatography and hydrophilic interaction liquid chromatography: Mixed mode behavior. *J. Chromatogr. A* **2012**, *1266*, 43–52. [[CrossRef](#)] [[PubMed](#)]
9. Ohshima, K.; Inoue, Y.; Kishikawa, N.; Kuroda, N. Preparation and characterization of surfactin-modified silica stationary phase for reversed-phase and hydrophilic interaction liquid chromatography. *J. Chromatogr. A* **2014**, *1371*, 257–260. [[CrossRef](#)] [[PubMed](#)]
10. Sander, L.C.; Wise, S.A. Synthesis and characterization of polymeric C18 stationary phases for liquid chromatography. *Anal. Chem.* **1984**, *56*, 504–510. [[CrossRef](#)]

11. Jinno, K.; Nagoshi, T.; Tanaka, N.; Okamoto, M.; Fetzer, J.C.; Biggs, W.R. Elution behaviour of planar and non-planar polycyclic aromatic hydrocarbons on various chemically bonded stationary phases in liquid chromatography. *J. Chromatogr. A* **1987**, *392*, 75–82. [[CrossRef](#)]
12. Silva, C.R.; Airoidi, C.; Collins, K.E.; Collins, C.H. Preparation and characterization of a new C₁₈ urea phase based on titanized silica. *J. Chromatogr. A* **2005**, *1087*, 29–37. [[CrossRef](#)] [[PubMed](#)]
13. Layne, J. Characterization and comparison of the chromatographic performance of conventional, polar-embedded, and polar-endcapped reversed-phase liquid chromatography stationary phases. *J. Chromatogr. A* **2002**, *957*, 149–164. [[CrossRef](#)]
14. Kučerová, G.; Kalíková, K.; Procházková, H.; Popr, M.; Jindřich, J.; Coufal, P.; Tesařová, E. Chromatographic Characterization of a New Cationic β -CD Based Stationary Phase Prepared by Dynamic Coating. *Chromatographia* **2016**, *79*, 529–536. [[CrossRef](#)]
15. Kakhki, R.M. Application of crown ethers as stationary phase in the chromatographic methods. *J. Incl. Phenom. Macrocycl. Chem.* **2013**, *75*, 11–22. [[CrossRef](#)]
16. Noguchi, H.; Takafuji, M.; Maurizot, V.; Huc, I. Chiral separation by a terminal chirality triggered P-helical quinoline oligoamide foldamer. *J. Chromatogr. A* **2016**, *1437*, 88–94. [[CrossRef](#)] [[PubMed](#)]
17. Zhang, C.; Ma, R.; Wang, H.; Sakai, R.; Satho, T.; Kakuchi, T.; Liu, L.; Okamoto, Y. Influence of Helical Structure on Chiral Recognition of Poly(phenylacetylene)s Bearing Phenylcarbamate Residues of L-Phenylglycinol and Amide Linage as Pendants. *Chirality* **2015**, *27*, 500–506. [[CrossRef](#)] [[PubMed](#)]
18. Fukumoto, T.; Ihara, H.; Sakaki, S.; Shosenji, H.; Hirayama, C. Chromatographic separation of geometrical isomers using highly oriented polymer-immobilized silica gels. *J. Chromatogr. A* **1994**, *672*, 237–241. [[CrossRef](#)]
19. Goto, Y.; Nakashima, K.; Mitsuishi, K.; Takafuji, M.; Sakaki, S.; Ihara, H. Selectivity enhancement of diastereomer separation in RPLC using crystalline-organic phase-bonded silica. *Chromatographia* **2002**, *56*, 19–23. [[CrossRef](#)]
20. Fowler, L.S.; Thomas, L.H.; Ellis, D.; Sutherland, A. A one-pot, reductive amination/6-endo-trig cyclisation for the stereoselective synthesis of 6-substituted-4-oxopipercolic acids. *Chem. Commun.* **2011**, *47*, 6569–6571. [[CrossRef](#)] [[PubMed](#)]
21. Berendsen, G.E.; Pikaart, K.A.; Galan, L. Preparation of various bonded phases for HPLC using monochlorosilanes. *J. Chromatogr.* **1980**, *3*, 1437–1464. [[CrossRef](#)]
22. Sander, L.C.; Pursch, M.; Wise, S.A. Shape Selectivity for Constrained Solutes in Reversed-Phase Liquid Chromatography. *Anal. Chem.* **1999**, *71*, 4821–4830. [[CrossRef](#)] [[PubMed](#)]
23. Jinno, K.; Kawasaki, K. Correlation between the Retention Data of Polycyclic Aromatic Hydrocarbons. *Chromatographia* **1983**, *17*, 445–449. [[CrossRef](#)]
24. Wise, S.A.; Bonnett, W.J.; Guenther, F.R.; May, W.E. A Relationship between Reversed-Phase C₁₈ Liquid Chromatographic Retention and the Shape of Polycyclic Aromatic Hydrocarbons. *J. Chromatogr. Sci.* **1981**, *19*, 457–465. [[CrossRef](#)]
25. Hemström, P.; Irgum, K. Hydrophilic interaction chromatography. *J. Sep. Sci.* **2006**, *29*, 1784–1821. [[CrossRef](#)] [[PubMed](#)]
26. Kahsay, G.; Song, H.; Schepdael, A.V.; Cabooter, D.; Adams, E. Hydrophilic interaction chromatography (HILIC) in the analysis of antibiotics. *J. Pharm. Biomed. Anal.* **2014**, *87*, 142–154. [[CrossRef](#)] [[PubMed](#)]
27. Wu, J.Y.; Bicker, W.; Linder, W. Separation properties of novel and commercial polar stationary phases in hydrophilic interaction and reversed-phase liquid chromatography mode. *J. Sep. Sci.* **2008**, *31*, 1492–1503. [[CrossRef](#)] [[PubMed](#)]
28. Verdolino, V.; Cammi, R.; Munk, B.H.; Schlegel, B. Calculation of pK_a Values of Nucleobases and the Guanine Oxidation Products Guanidinohydantoin and Spiroiminodihydantoin using Density Functional Theory and a Polarizable Continuum Model. *J. Phys. Chem. B* **2008**, *112*, 16860–16873. [[CrossRef](#)] [[PubMed](#)]
29. Deng, S.; Hou, G.; Xue, Z.; Zhang, L.; Zhou, Y.; Liu, C.; Liu, Y.; Li, Z. Vitamin E isomer δ -tocopherol enhances the efficiency of neural stem cell differentiation via L-type calcium channel. *Neurosci. Lett.* **2015**, *585*, 166–170. [[CrossRef](#)] [[PubMed](#)]

